Experimental investigation of droplet collisions with higher viscosity

Matthias Kuschel*, Martin Sommerfeld
Mechanische Verfahrenstechnik
Martin-Luther-Universität Halle-Wittenberg
D-06099 Halle (Saale), Germany

Abstract

The present work focuses on the investigation of binary droplet collisions consisting of solutions with different mass fraction of solids. The increase of solids content is associated with a remarkable increase in viscosity. In order to generate mono-disperse droplets two fine liquid jets are excited by means of piezo-electric generators causing a controlled break-up. The impact parameter and the relative velocity included in the We-number are changed systematically. The methodical part will concentrate on a different method to describe the tracking of the droplets to determine the relative velocity and the resulting trajectory of the colliding droplets. Mass fraction and hence viscosity have a great influence on the collision outcome and cause a shift of the impact parameter–Weber number–diagram (B–We–diagram) towards higher Weber numbers [3].

Introduction

During the last decades many experiments on droplet collisions were carried out with different types of liquids [1, 2, 3, 4, 5, 6, 7]. Nearly all of them had in common, that they used roughly the same range of rather low viscosity (i.e. 1-5 mPa s) for their experiments. Jiang et al.[6] recognized that alkanes with different viscosities caused a shift of the boundary curves between the different collision outcomes towards higher We-numbers. Kurt [6] was one of the first who studied the influence of solid particles in suspensions on the collision behaviour. We want to step back slightly by analysing the influence of the solids content in solutions.

This work aims at investigating a wider range of viscosity for different polymerized Polyvinylpyrolindones-PVP (1-Ethenyl-2-pyrrolidone) with respect to the collision outcome.

Materials and Methods

Experimental Work

The experiments were carried out by using two piezo-electric droplet generators. The angle between the droplet chains and the pressure were varied in order to change the relative velocity in a range of 0.5 to 3.5 m/s. The liquid was pressed through the nozzle (producer: encap biosystems) with a diameter of 200 µm, resulting in droplets of around 380 µm in size. The temperature was kept constant at about 22°C by a thermostat. The Impact parameter was modified by using the *aliasing* method (frequency shift) [4]. Two CCD-cameras were used, observing the collision under an angle of 90° (front view or collision plane and side view). Figure 1 illustrates the experimental setup. By using two cameras it was possible to assure that the collision occurs in one plane, so that errors caused by off-centre impacts were avoided to a large extent.

The high-speed camera (type: 1200 HS from PCO AG), observed the collision event from the front side, so that all relevant parameters were detectable. The effect of an increasing mass fraction was investigated. The range of the PVP mass fraction was between 10 and 30 Ma %. The flight of the droplets and the collision were recorded by the high speed camera with around 6000 fps to have the process time resolved. This approach allows for every droplet pair to be assigned to the corresponding regime. The perpendicular positioned camera was a double shutter CCD-camera (PCO Sensicam) to ensure proper alignment of the collision plane. Additionally, it is possible to observe the deformation of the droplet contour and the creation of satellite droplets.

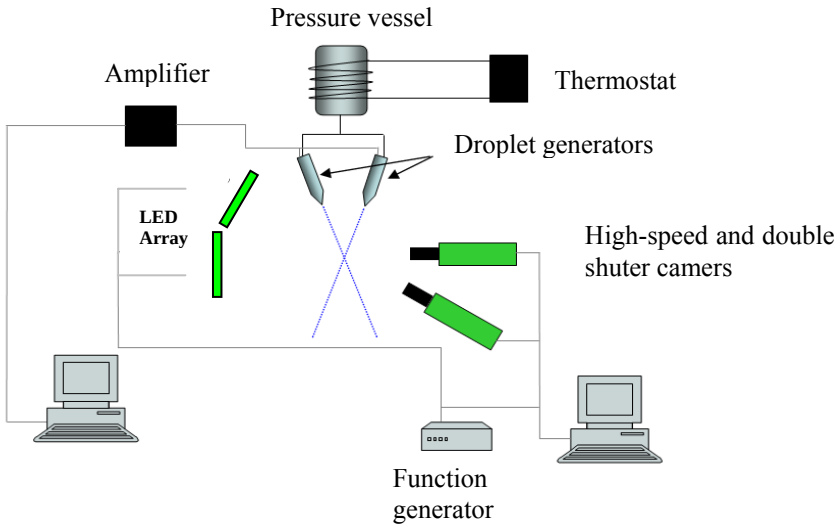

Figure 1. Sketch of the experimental setup

Tracking of droplets

The particle tracking has an underlying contour detecting algorithm which processes the raw images by applying a gradient filter and a binarizing filter to the images. Subsequently, the sharp edges of the contour are detected and transformed into positions in the image. By means of the positions of the contour points it is possible to calculate the droplet centres, which are compared between two subsequent pictures yielding the velocity of the droplet.

In the experiment the droplets fly, if the jet is excited properly, on a straight path, which can be described by a linear regression of the centres of gravity of the droplets. In practice however, the velocity vectors measured via image analysis are slightly fluctuating. This implies that the collision point also fluctuates, with the result that the impact parameter for a given geometry of the collision event will vary.

If one assumes the linear regression as the real trajectory or direction of flight one can derive the real impact parameter by calculating the normalized regression vector multiplied with the measured velocity vector. This yields the velocity of the droplet in direction of the trajectory (Fig. 2).

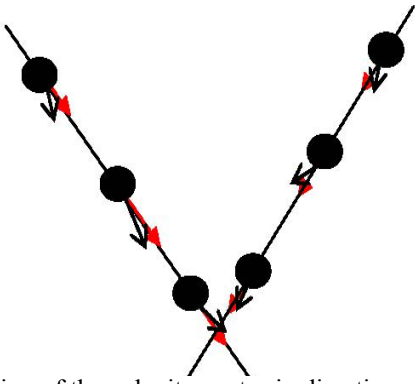

Figure 2. Sketch of the correction of the velocity vector in direction of the averaged direction of flight; not filled arrows: measured velocity vector; filled arrows: corrected direction of flight

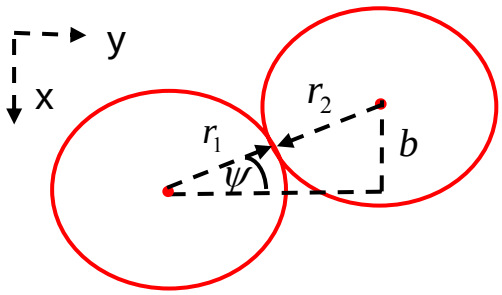

Figure 3. Definition of the impact parameter B

The calculation of the impact parameter was done as suggested by Kurt [6].

$$B = \frac{b}{r_1 + r_2} = \sin\psi \tag{1}$$

The collision Weber number is given by:

$$We = \frac{\rho_l \; D_d \; \vec{U}_{rel}^{\,2}}{\sigma_l}$$

$$D_d - Droplet\ diameter\ of\ the\ smaller\ droplet \tag{2}$$

$$\vec{U}_{rel} - relative\ velocity$$

$$\rho_l - Density\ of\ the\ fluid\,; \quad \sigma_l - Surface\ tension$$

The smaller droplet has been chosen, but the difference of the radii was below 10 µm, causing a difference of max. 3 %.

Relative velocity

Starting from the momentum conservation law for plastic impacts the first equation (3) has to be solved. This equation can be split into the two directions in space (Eq. 5 and 5) and therefore the relative velocity and the resulting flight vector can be determined. The angle $\mathrm{Cos}(\alpha_3)$ can be replaced by (Eq. 6), so that the two equations (Eq. 4 and 5) are sufficient to find a solutions. The relative velocity is only composed of the normal components of the two vectors u_1, u_2. A schematic plot regarding the velocity determination is shown in figure 4.

$$m_1\, u_1 + m_2\, u_2 = (m_1 + m_2)\, u_3 \tag{3}$$

$$m_1\, u_1\, \mathrm{Sin}(\alpha_1) + m_2\, u_2\, \mathrm{Sin}(\alpha_2) = (m_1 + m_2)\, u_3\, \mathrm{Sin}(\alpha_3) \tag{4}$$

$$m_1\, u_1\, \mathrm{Cos}(\alpha_1) + m_2\, u_2\, \mathrm{Cos}(\alpha_2) = (m_1 + m_2)\, u_3\, \mathrm{Cos}(\alpha_3) \tag{5}$$

$$\mathrm{Cos}(\alpha_3) = \sqrt{1 - \mathrm{Sin}(\alpha_3)^2} \tag{6}$$

m_1, m_2 mass of droplet 1 and 2 [kg]
u_1, u_2 velocity of droplet 1 and 2 [m/s]
α_1, α_2, α_3 angles between the x axis and u_1, u_2, u_3 [°]

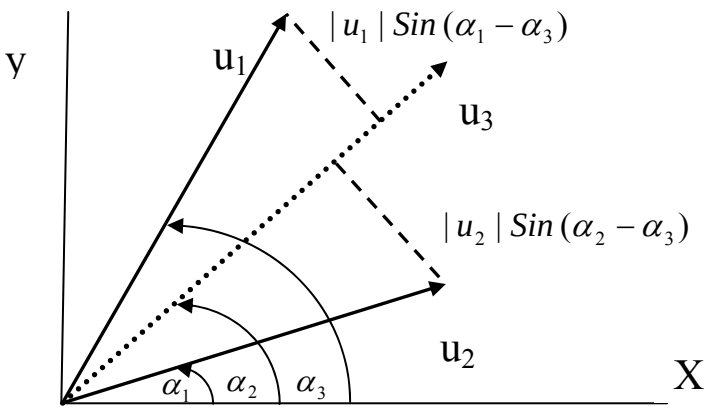

Figure 4. Relative velocity vector after collision; the collision point is in the origin of the coordinate system

Results and Discussion

In Figures 5 and 6 the comparison between the droplet motion simulated by the tracking method mentioned above and the experiment is shown. The pictures Fig. 5 a) and b) were used to determine the velocities and the regression vector. Pictures 5 c) and d) show the impact of the marked droplets from figure 5 a). Figures 6 c) and d) illustrate the simulated droplet motion. The new tracking method shows very good agreement with the experiment and proves that the impact parameter is also correctly calculated for drops which are more far away from the actual collision point. The marked droplets of picture 5 a) are also depicted in Figure 6 a) to show the droplets belonging together more clearly.

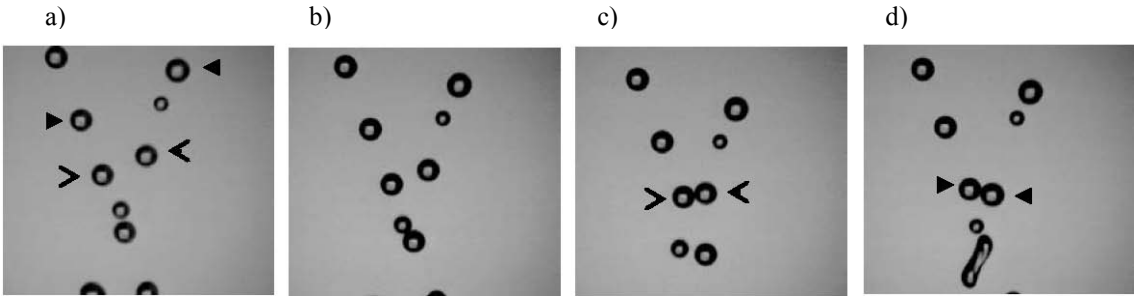

Figure 5: Pictures a) and b) were used to determine the velocity of the droplets; droplets marked with arrow heads of same shape will collide with each other; c) and d) show the impact of the droplets from the first picture.

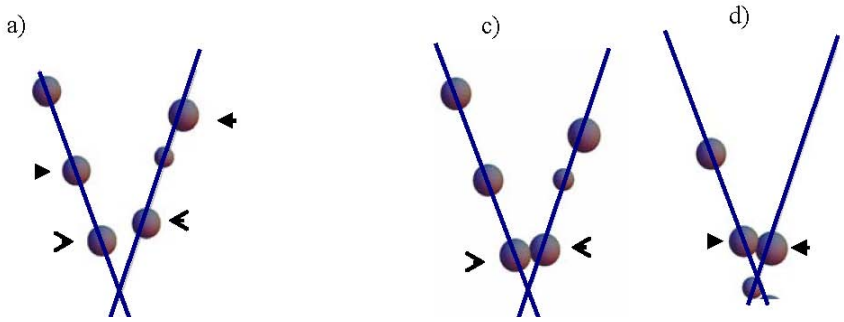

Figure 6. Simulated droplet impacts using the new tracking method.

The experiments were carried out as described above. In addition to the dissolved polymer solutions of different mass fraction distilled water was investigated for comparison. All known collision outcomes could be found during the measurements, namely bouncing, coalescence, stretching and reflexive separation. Normally, bouncing occurred only at high impact parameters. For water (Fig. 7) coalescence was found over the whole B-range for very small We-numbers, caused by an increased contact time.

With increasing We- numbers the fraction of coalescence decreased and stretching separation took place starting from We ≈ 18. The boundary between stretching separation and coalescence found from the present measurements is located at somewhat lower impact parameters as predicted by the analytical solution obtained by Ashgriz & Poo [1] while reflexive separation is over predicted by the solution. This result differs from literature findings, which might be explained through more precise adjustment of the droplet chains with respect to each other by using the second CCD camera in order to insure that the droplets collide exactly in one plane. Moreover, a single droplet tracking method was used to determine the collision outcome and the collision point accurately.

In the following the results for PVP with different mass fractions will be presented and discussed. Already a small mass fraction results in a completely different collision map compared to water (see Fig. 7 and 8). Bouncing and stretching separating are shifted downwards smaller impact parameters. As a result, the region of coalescence decreases and is limited to $B < 0.3$. The region of reflexive separation increased compared to the water case. From the three diagrams (Fig. 8 – 10) a general clear trend is observed, namely a shift of the regimes boundaries towards higher We-numbers. Furthermore, a shift of the bouncing region towards lower We-numbers is observed and eventually at higher solids content bouncing extends over the whole range of B ($0 < B < 1$). The region of stretching separation shifts clearly to higher Weber numbers and impact parameters. At low mass fractions of the polymer solution reflexive separation was an additional outcome, which vanished at 30 Ma% PVP. A possible reason for the shift to higher We-numbers could be the increasing viscosity (implicit) with the solids content, resulting in different collision behaviour (Table 1).

Since the relative velocity was in the same order for all the experiments, the slightly increasing ratio of liquid density to the surface tension also yields a shift to higher We-numbers (Table 1). Interestingly, the shape of the regimes remains more or less similar to those observed for water, although the properties of the solutions are different.

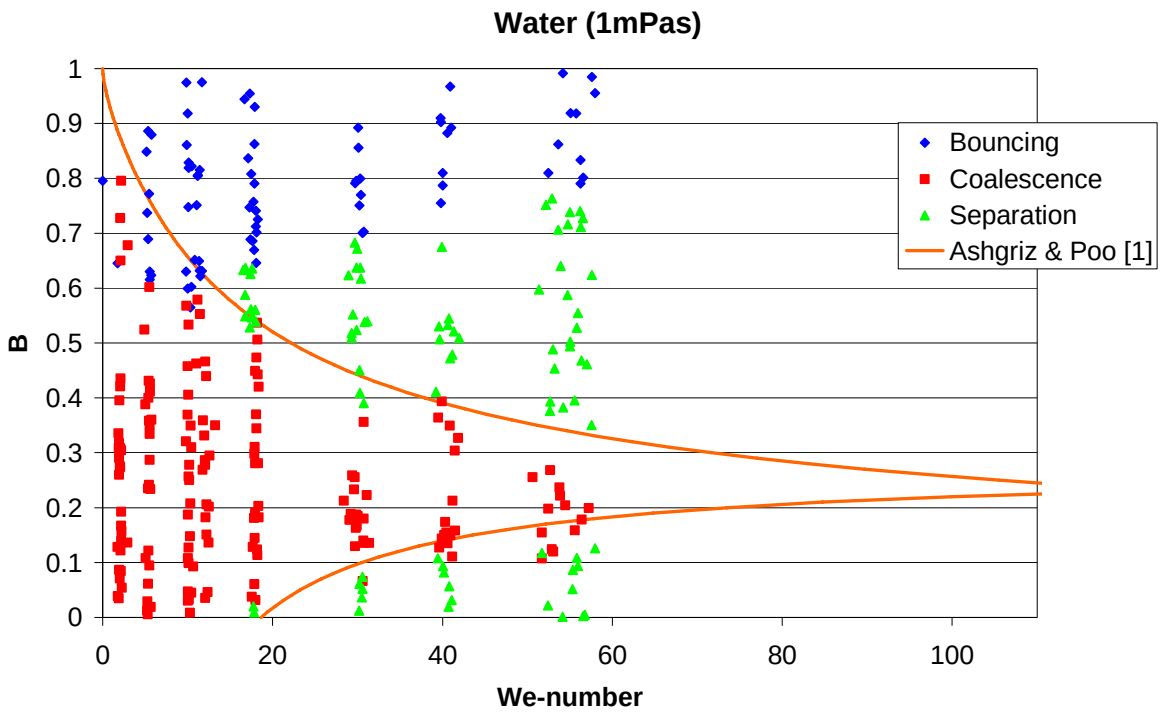

Figure 7. Impact – Weber – diagram for water

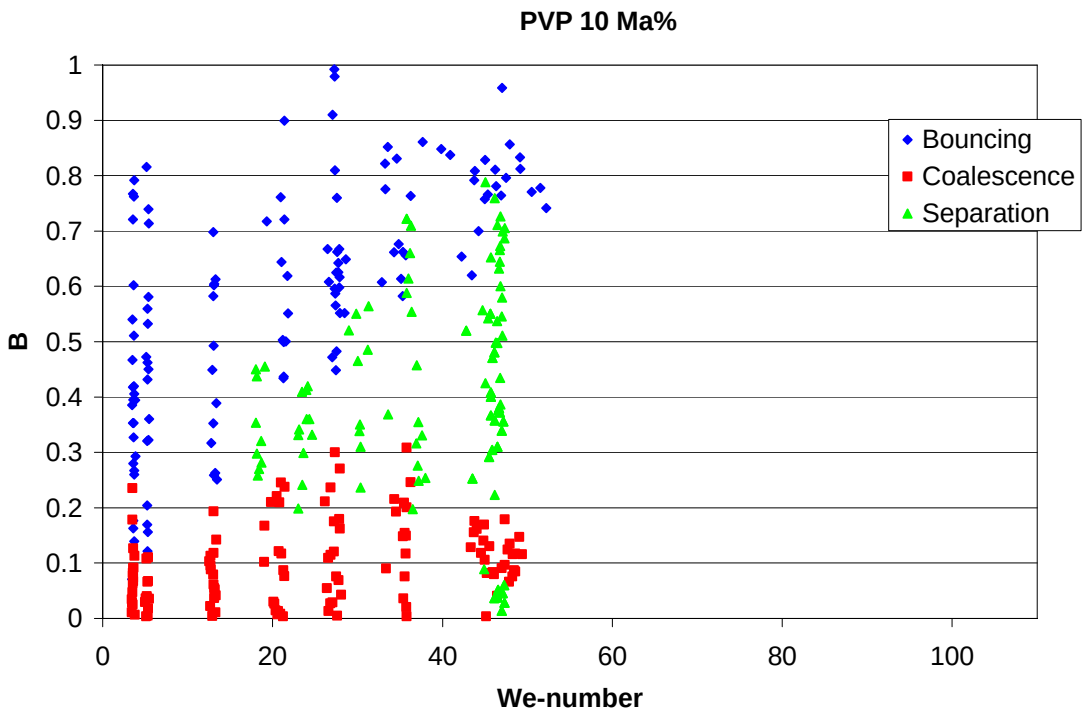

Figure 8. Impact – Weber – diagram for K17 with 10 Ma% solids content

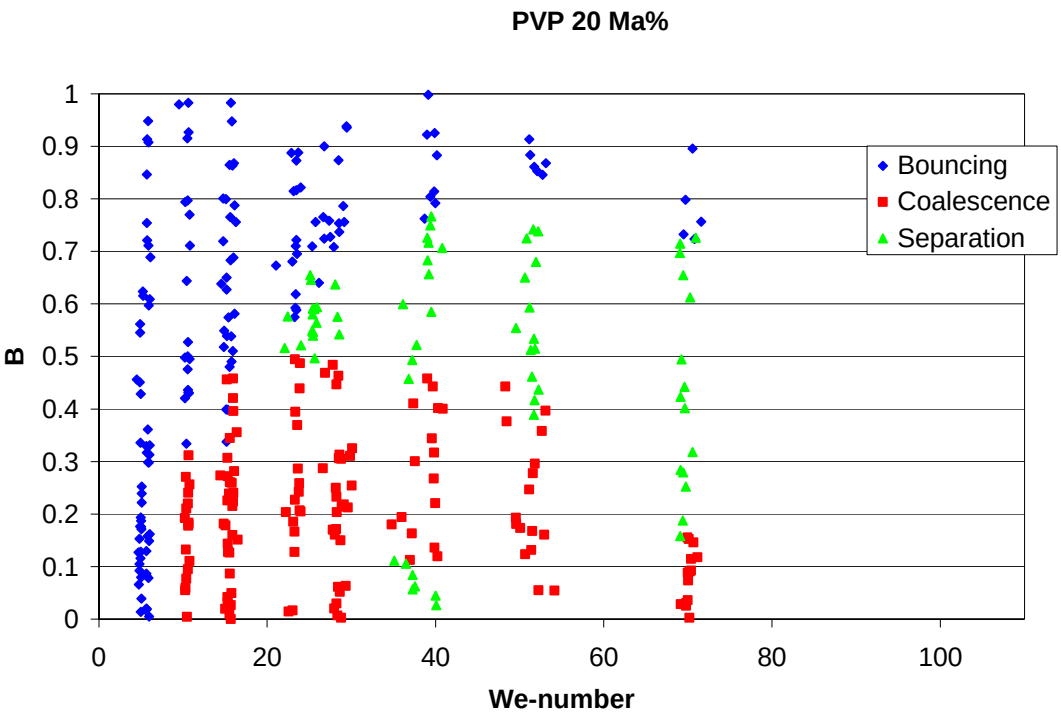

Figure 9. Impact – Weber – diagram for K17 with 20 Ma% solids content

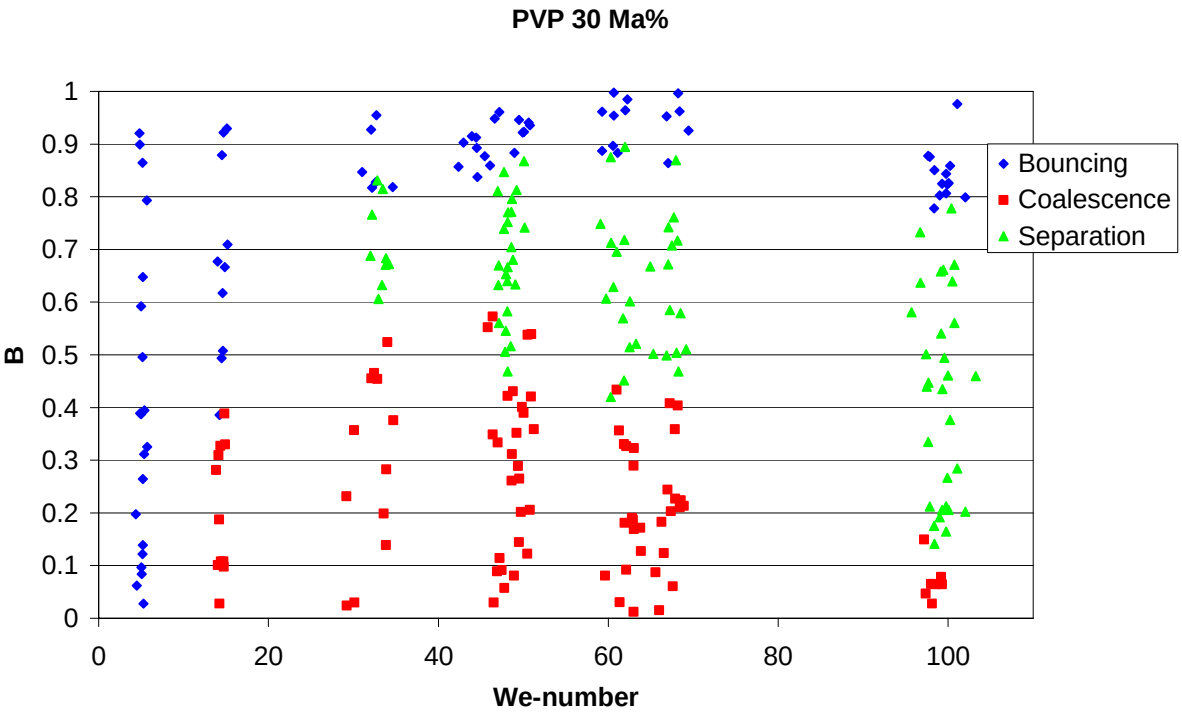

Figure 10. Impact – Weber – diagram for K17 with 30 Ma% solids content

Table 1. Surface tension measured with dataphysics oca 20 (hanging drop)

Species & Solids content	Surface tension [mN/m]	Density [kg/m^3]	Viscosity [mPas]
Water	72.7	998.2	0.95
K17 10Ma%	69.1	1019.5	2.35
K17 20 Ma%	67.4	1046.1	6.01
K17 30 Ma%	66.3	1064.8	15.41

Conclusion

The collision outcome for solution droplets (PVP) with different solids content was experimentally studied using two piezo-electric droplet generators, which produce two droplet chains with roughly identical size. The time resolved droplet collisions and the perpendicular adjustment of two CCD-cameras assure a correct determination of the impact point and the collision outcome. For calculating the relative velocity and the impact point (impact parameter) a droplet tracking method was used by ensuring a common flight direction of all droplets in the chain. The observed impact point agreed very well with the tracking simulation.

Measurements were conducted for water and solutions with different solids mass fractions and the collision maps (B-We-diagrams) were constructed. All typical collision scenarios, i.e. bouncing, coalescence, stretching separation and reflexive separation were observed. A shift of the collision regimes towards higher We-numbers was found for increasing solids content and hence solution viscosity. This implies, that the region of bouncing is enlarged and extends over the entire impact parameter range at small We-numbers and higher solids content.

The following task will be a systematic classification of the regime by formulating the physical behaviour. In a next step existing models will be compared with the data and probably adapted.

Acknowledgement

The authors acknowledge the financial support of this research project by the Deutsche Forschungsgemeinschaft (DFG) under contract SO 204/35-1.

Additionally we want to thank the University of Kiel - Institut für Humanernährung und Lebensmittelkunde - Abteilung Lebensmitteltechnologie for the cooperation in determining PVP characteristics.

References

[1] Ashgriz, N.; Poo, J.Y.:"Coalescence and separation in binary collisions of liquid drops", *Journal of Fluid Mechanics* 221:183-204 (1990).

[2] Brenn, G., Kolobaric, V. "Satellite droplet formation by unstable binary drop collisions", *Physics of Fluids*, 18, 087101-1 – 18 (2001).

[3] Estrade, J.-P., Carentz, H., Lavergne, G., Biscos, Y. "Experimental investigation of dynamic binary collision of ethanol droplets - a model for droplet coalescence and bouncing", *International Journal of Heat and Fluid Flow* 20, 486-491 (1999).

[4] Gotass , C., Havelka, P. Jakobson, H. A. and Svendsen H.F.: "Evaluation of the impact parameter in droplet droplet collision experiments by the aliasing method", *Physics of Fluids* 19:102105 (1-11) (2007)

[5] Jiang, Y. J., Umemura, A. and Law, C.K.: "An experimental investigation on the collision behavior of hydrocarbon droplets", *Journal of Fluid Mechanics* 234:171-190 (1992).

[6] Kurt, O., Fritsching, U. and Schulte, G.: "Binary Collisions of Droplets with Fluid and Suspension Particles", *21th ILASS* 2007.

[7] Qian, J. and Law,C.K.:"Regimes of coalescence and separation in droplet collision", *Journal of Fluid Mechanics* 331:59-80 (1997).